

SPECTROPHOTOMETRY OF BETA LYRAE

Theodore E. Houck
University of Wisconsin
Madison, Wisconsin

Two hundred and fourteen scans over the wavelength region 1100 Å to 1800 Å with 10 Å resolution were obtained for the eclipsing binary Beta Lyrae between JD 2440889.5 and JD 2440904.5. The scans were made regularly at 100 minute intervals corresponding to 0.0054 intervals of the binary's cycle and extend from phase -0.245 to +0.912. Exposure times were 8 seconds per 10 Å step. Correcting for the 1/64 prescaler, the count rate was typically of the order of 16,000 counts per exposure at 1800 Å decreasing to about 300 counts per exposure in the vicinity of Lyman alpha, both measures above a typical background count of 300 counts per exposure. Except at primary and secondary minima (where the star was too faint), the OAO spacecraft was kept under Boresight Tracker control to reduce wavelength shifts in the objective grating spectrometer due to errors in pointing to less than 1 Å and all scans were made in the same direction, 1800 Å to 1100 Å, to reduce effects of backlash in the grating drive, the scanner being reset to the long wavelength end while the star was being occulted by the earth. All scans were made while the spacecraft was in the earth's shadow and the extinction of the star by the earth's atmosphere could be observed during the reverse resetting scan.

While computer reduction of the resulting 18,000 measurements is still in progress, some preliminary results can be indicated. Figure 1 shows the average of four successive scans near primary minimum compared with four scans at phase 0.25 and similarly Figure 2 compares a four scan average near secondary minimum with the average scan at phase 0.25. In all cases the scans have been corrected for a possible variable background count by using the dark readings of Stellar Photometer No. 2 to monitor the effects of the radiation belt, and a preliminary calibration of the spectrometer has been applied to reduce the raw data to a relative energy per unit wavelength. It should be emphasized that because of the preliminary nature of the calibration for the spectrometer, the resulting curves may be in error, particularly at the short wavelength end, but since the same calibration reduction was made to all data pre-

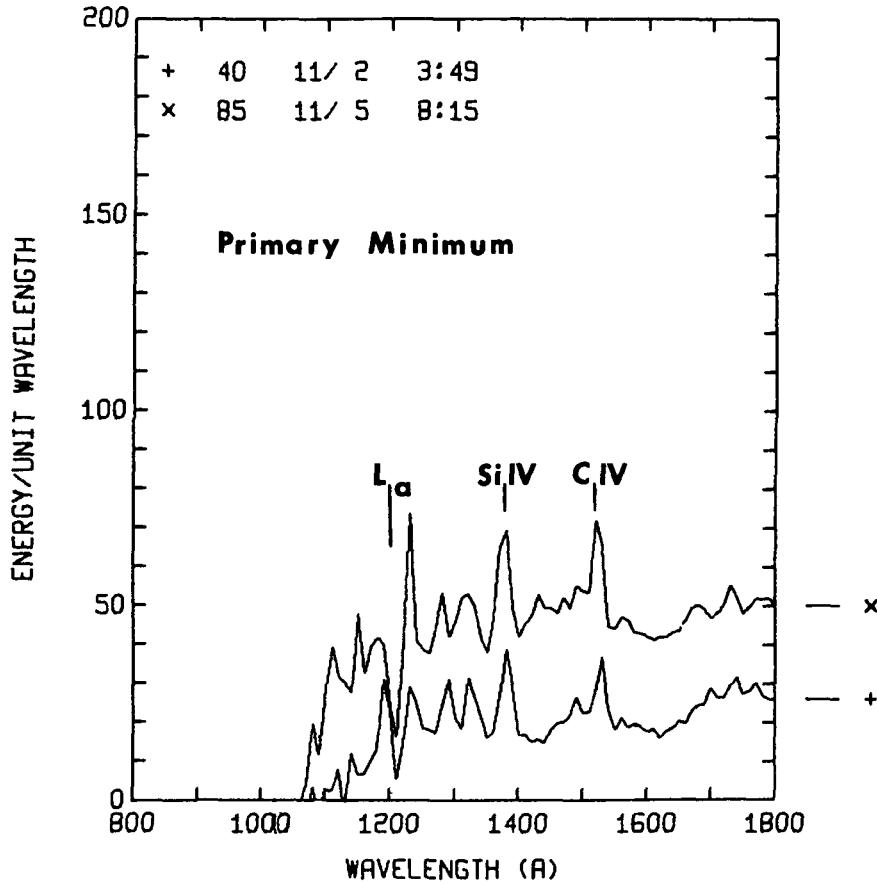


Figure 1.

sented here, a relative comparison of the scans remains valid. The data in the upper left corners of Figures 1 and 2 are simply a running number identifying the first scan of the four scan average and the GMT month, day, hour and minute of the average scan or the center point of the 0.021 phase interval covered by the four scans.

Several points are illustrated by Figures 1 and 2.

1. The intensity at primary minimum is almost exactly one-half that at maximum, i.e., over the wavelength region covered, the primary eclipse is less deep than in the visual or longer ultraviolet wavelengths. This trend is also shown in simultaneous filter photometry light curves of the following paper (Kondo, McCluskey and Houck 1972).

2. Except for the 1100-1200 Å region, the depth of the primary eclipse appears remarkably independent of wavelength. It should be remembered that for the 1100-1200 Å region the signal is less than the background noise and a small error in

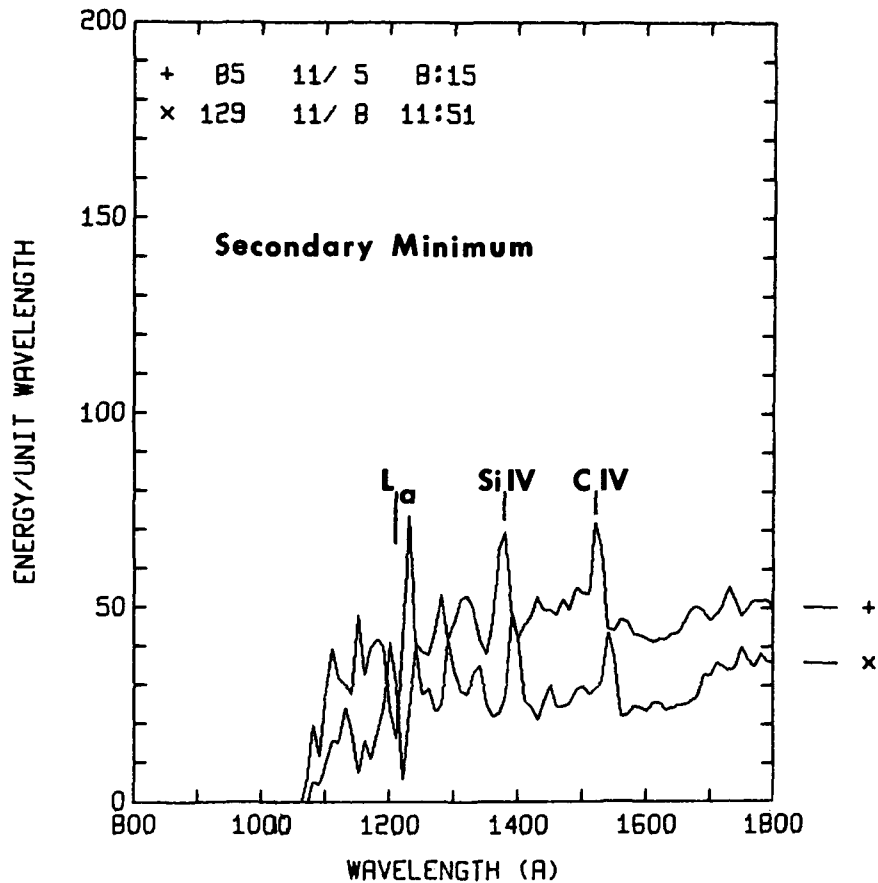


Figure 2.

the latter will more seriously affect the reduced curve.

3. The energy distribution at secondary minimum is similar to that at primary and again about half that of maximum and similarly independent of wavelength; thus, the secondary eclipse cannot be a geometric eclipse of a star of later spectral type than the primary whose energy distribution approximates that of a normal star.

4. While identification of spectral lines at a 10 \AA resolution is difficult, the two most prominent emission lines, other than the features near Lyman α , match well both in position and intensity with Si IV and C IV emission observed in the Wolf-Rayet star $\gamma \text{ Vel}$, and if so would seem to imply an exciting source of rather high temperature.

5. As can be seen in Figures 1 and 2, the emission lines, other than the features near Lyman α , do not show appreciable variation with phase and must therefore arise from a region which is largely unaffected by the geometrical eclipse.

The primary variation in the scans is the feature near the interstellar Lyman α . This is shown in more detail in Figure 3 which shows a sample of four scan averages from 1100-1400 \AA , with the phase indicated in degrees. The interstellar Lyman α absorption line is indicated, and on either side there appear to be emission features which vary with phase from 0° to 180° and are relatively constant from 180° to 360° . It should be remembered that with the 10 \AA resolution, the line profiles are essentially instrumental, and do not represent the true profiles of the star. With the low resolution of the spectrometer one cannot rule out the possibility that the features of interest arise from variable spectral lines adjacent to Lyman α , but it is exceedingly tempting to interpret them as arising from an interplay between the interstellar Lyman α absorption line and a broad emission Lyman α line in β Lyrae which is Doppler shifted by the varying geometry of the system.

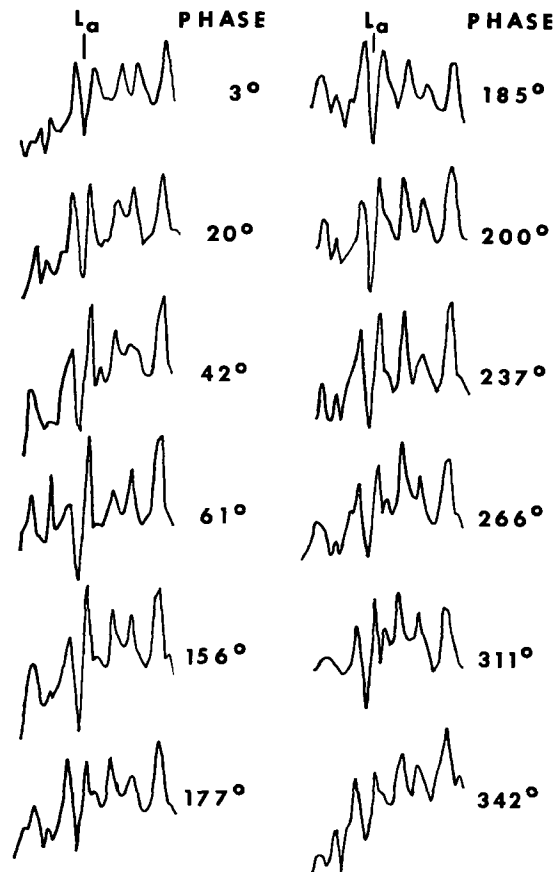


Figure 3.

Suppose the assumed Lyman α emission has a comparable width because of Doppler broadening to the interstellar line, then a portion of the emission line will lie in the wings of the interstellar line where the absorption is less than unity and can be detected by the low resolution spectrometer. If the radial velocity of the emission matches that of the interstellar absorption, equal intensities would be observed on either side of the center wavelength. If the emission line as a whole is now Doppler shifted in either direction, a corresponding increase in intensity will be observed on the appropriate side of the center wavelength even if the resolution of the spectrometer is low compared to the Doppler wavelength shift. In short, the interstellar line acts as a discriminator converting the frequency modulated Lyman α emission into an amplitude modulated signal of the low resolution spectrometer. Ideally if the instrumental profile is known with sufficient accuracy, and the interstellar absorption profile is also known with comparable accuracy, radial velocity effects can then be measured where the wavelength shift is considerably smaller than the wavelength resolution of the detecting spectrometer. The alternative interpretation that the emission feature on the longward side of Lyman α results from a variation in strengths of other lines such as N V, 1240 Å, is far less attractive. It would require a very asymmetric spatial or temporal variation not shared by any other line in the spectrum of β Lyrae.

Since the scans in the vicinity of Lyman α show primarily emission features and the location of the continuum is uncertain, Figure 4 shows a plot of L/S vs. phase of β Lyrae, where L equals the height of the longward emission feature above the bottom of the interstellar Lyman α core and S is the height of the shortward feature. By choosing the interstellar Lyman α core as a reference, a direct quantitative interpretation is difficult, but the figure does show that the variation is well correlated with the phase of the binary system. The dots and crosses in the figure separate the overlap in the observations beyond a single cycle of the binary system. The figures at the top indicate the orientation of the system where the primary is defined as the object producing the spectral lines in the visual used to determine the radial velocity curve of the system as a spectroscopic binary.

One might end with the speculation that if the variation in features observed is correctly interpreted as resulting from Doppler shifted Lyman α , Figure 4 would seem to imply that either there is a strong local influx of hydrogen on the "back-side" of the secondary with velocities of the order of several hundred km/sec which is obscured between phase 180° - 360° by the secondary, or that the shortward shifted Lyman α emission is selectively absorbed within the cloud surrounding the binary system.

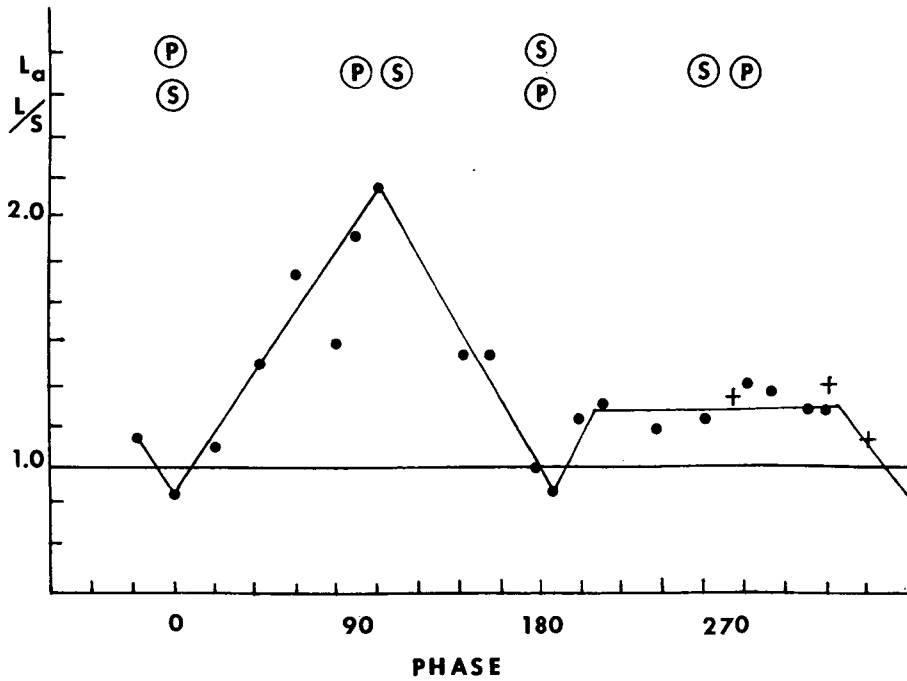


Figure 4.

The author is highly indebted to Mr. T. Jones for the computer programs involved in generating Figures 1-3, and to NASA and Grumman personnel for the existence and operation of the spacecraft.

REFERENCES

Kondo, McCluskey and Houck 1972, *this volume*.